

The EKV Normalized Functions

For the Design of Analog Circuits (Version 1)

Christian Enz (christian.enz@epfl.ch)

2025-09-30

Table of contents

| | | |
|----------|---|-----------|
| 1 | Introduction | 3 |
| 2 | Large-signal functions | 4 |
| 2.1 | Normalized current versus charge | 4 |
| 2.1.1 | Long-channel | 4 |
| 2.1.2 | Short-channel | 4 |
| 2.2 | Normalized charge versus current | 5 |
| 2.3 | Normalized saturation voltage versus charge | 5 |
| 2.4 | Normalized saturation voltage versus inversion coefficient | 7 |
| 2.5 | Normalized charge versus saturation voltage | 7 |
| 2.6 | Inversion coefficient versus saturation voltage | 8 |
| 2.7 | Drain-to-source saturation voltage versus inversion coefficient | 8 |
| 2.8 | Inversion coefficient versus drain-to-source saturation voltage | 9 |
| 2.9 | Slope factor versus inversion coefficient | 9 |
| 3 | Small-signal functions | 11 |
| 3.1 | Inversion coefficient versus transconductance | 12 |
| 3.2 | Normalized G_m/I_D versus inversion coefficient | 12 |
| 3.3 | Inversion coefficient versus normalized G_m/I_D | 13 |
| 3.4 | Noise functions | 13 |
| 3.4.1 | Thermal noise | 13 |
| 4 | Normalized intrinsic capacitances | 16 |
| | References | 18 |

1 Introduction

This notebook presents all the normalized functions that are used for the design of analog circuits using the G_m/I_D approach with the inversion coefficient [1] [2] [3] [4].

2 Large-signal functions

2.1 Normalized current versus charge

2.1.1 Long-channel

The normalized drain current or inversion coefficient IC is defined as the drain current in saturation normalized to the specific current I_{spec}

$$IC \triangleq \frac{I_D|_{saturation}}{I_{spec}}, \quad (2.1)$$

where the specific current is given by

$$I_{spec} = I_{spec\Box} \cdot \frac{W}{L} \quad (2.2)$$

with

$$I_{spec\Box} \triangleq 2n \cdot \mu \cdot C_{ox} \cdot U_T^2. \quad (2.3)$$

The inversion coefficient IC gives the level of inversion of the transistor according to

$$IC < 0.1 \text{ weak inversion (WI)}, \quad (2.4)$$

$$0.1 \leq IC < 10 \text{ moderate inversion (MI)}, \quad (2.5)$$

$$10 \leq IC \text{ strong inversion (SI)}. \quad (2.6)$$

The inversion coefficient for a long-channel transistor is a function of the normalized source charge according to

$$IC = q_s^2 + q_s \quad (2.7)$$

where q_s is the inversion charge Q_i evaluated at the source and normalized to $Q_{spec} \triangleq -2nC_{ox}U_T$

$$q_s \triangleq \frac{Q_i(x=0)}{Q_{spec}}. \quad (2.8)$$

The expression of IC versus q_s can be inverted to express the normalized charge as a function of the inversion coefficient according to

$$q_s = \frac{\sqrt{4IC + 1} - 1}{2} \quad (2.9)$$

2.1.2 Short-channel

The normalized drain current in the simplified EKV (sEKV) model is given by

$$IC \triangleq \frac{I_D|_{saturation}}{I_{spec}} = \frac{2(q_s^2 + q_s)}{1 + \sqrt{1 + \lambda_c^2(q_s^2 + q_s)}}, \quad (2.10)$$

where parameter λ_c is the velocity saturation parameter which scales as

$$\lambda_c = \frac{L_{sat}}{L} \quad (2.11)$$

where $L_{sat} = 2\mu U_T/v_{sat}$ is the length over which the carriers velocity is saturating to v_{sat} . λ_c is therefore the fraction of the channel over which the carriers are in full velocity saturation. The long-channel case is obtained by setting $\lambda_c = 0$ for which the normalized drain current (2.10) reduces to (2.7).

The short-channel asymptotes are given by

$$IC \cong \begin{cases} q_s & \text{in weak inversion } (\lambda_c \cdot q_s \ll 1), \\ \frac{2q_s}{\lambda_c} & \text{in strong inversion } (\lambda_c \cdot q_s \gg 1). \end{cases} \quad (2.12)$$

The inversion charge IC is plotted versus q_s in Figure 2.1 for the long- and short-channel cases.

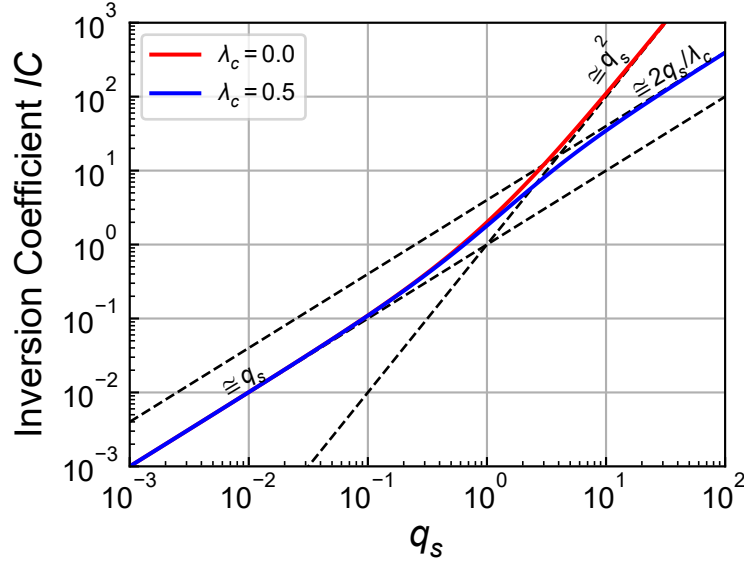


Figure 2.1: Inversion coefficient IC versus normalized source charge q_s .

2.2 Normalized charge versus current

Equation (2.10) can be inverted to express the normalized source charge in function of the inversion coefficient

$$q_s = \frac{\sqrt{4IC + 1 + (\lambda_c IC)^2} - 1}{2} \quad (2.13)$$

which for long-channel ($\lambda_c = 0$) reduces to

$$q_s = \frac{\sqrt{4IC + 1} - 1}{2}. \quad (2.14)$$

The normalized source charge q_s is plotted versus the inversion coefficient IC in Figure 2.2 for both the long- and short-channel cases.

2.3 Normalized saturation voltage versus charge

The charge is related to the voltage according to

$$v_p - v_s = 2q_s + \ln(q_s) \quad (2.15)$$

which is plotted which is plotted in Figure 2.4.

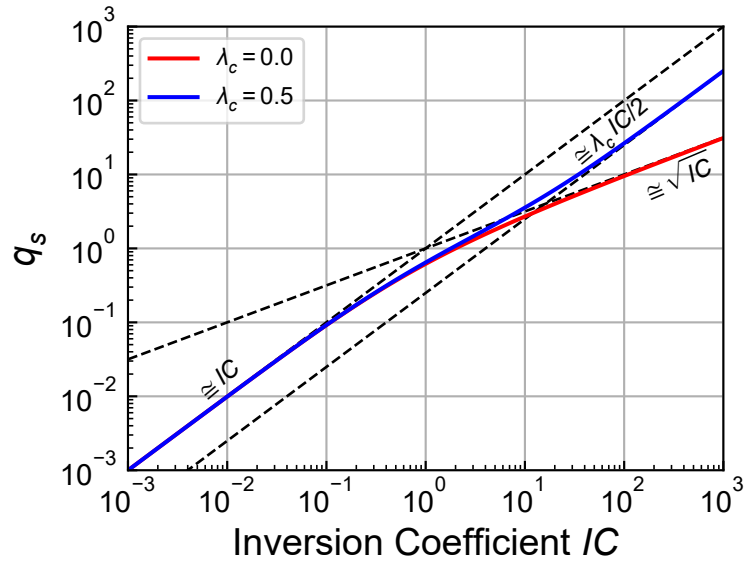


Figure 2.2: Normalized source charge q_s versus inversion coefficient IC .

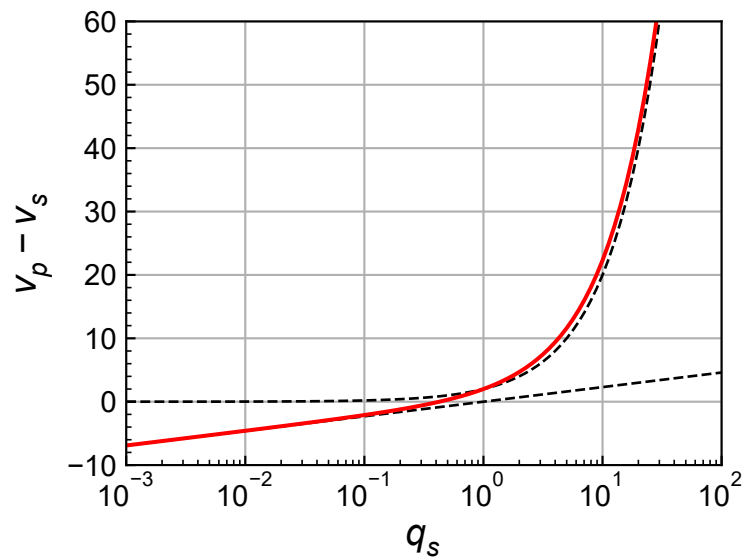


Figure 2.3: Normalized saturation voltage $v_p - v_s$ versus normalized source charge q_s .

2.4 Normalized saturation voltage versus inversion coefficient

The source charge can be expressed in terms of the inversion coefficient as (2.14) for a long-channel transistor or (2.13). Replacing in (2.15) allows to express the saturation voltage in terms of the inversion coefficient. For a long-channel transistor we get

$$v_p - v_s = \ln(\sqrt{4IC + 1} - 1) + \sqrt{4IC + 1} - 1 - \ln(2) \quad (2.16)$$

The saturation voltage $v_p - v_s$ is plotted versus the inversion coefficient IC in Figure 2.4 for both the long- and short-channel case.

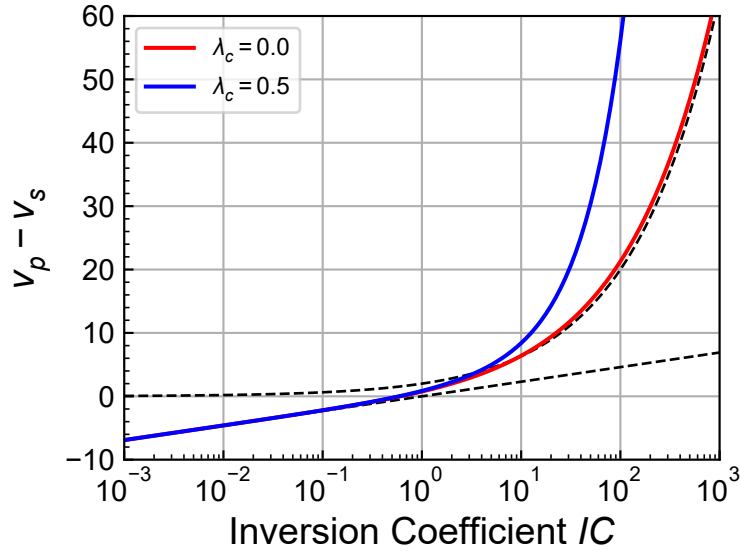


Figure 2.4: Normalized saturation voltage $v_p - v_s$ versus inversion coefficient IC .

2.5 Normalized charge versus saturation voltage

The voltage versus charge equation (2.15) can actually be inverted using the Lambert W-function of order 0. The Lambert function $W(z)$ is defined as the function satisfying

$$W(z) \cdot e^{W(z)} = z. \quad (2.17)$$

The voltage versus charge equation can be written as

$$2q \cdot e^{2q} = e^v \quad (2.18)$$

where $q \triangleq q_s$ and $v \triangleq v_p - v_s$. Eqn. (2.18) can now be solved for q using the Lambert W-function by setting $z = 2e^v$ which leads to

$$q(v) = \frac{1}{2} W(2e^v) \quad (2.19)$$

or

$$q_s = \frac{1}{2} W(2e^{v_p - v_s}). \quad (2.20)$$

The Lambert W-function is available in the *scipy* Python package as *lambertw*. It is also available in Mathematic as the *ProductLog[z]* function.

The charge versus voltage can also be approximated by the EKV function which is compared to the exact Lambert W-function in Figure 2.5.

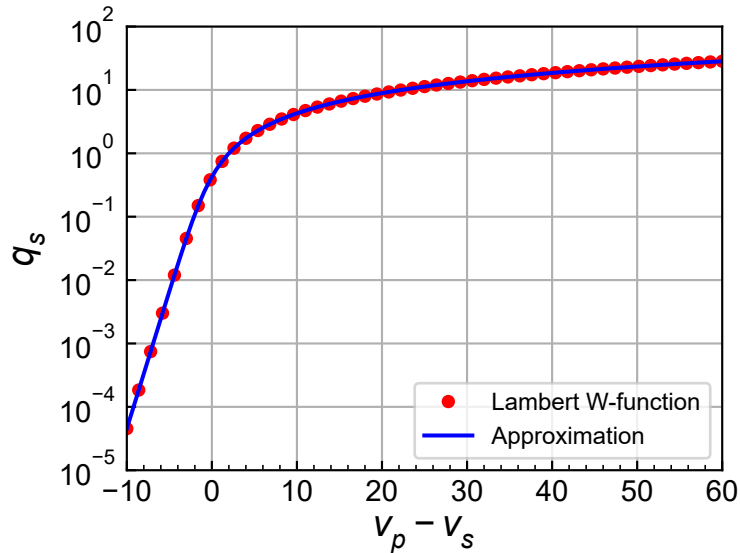


Figure 2.5: Normalized source charge q_s versus normalized saturation voltage $v_p - v_s$.

2.6 Inversion coefficient versus saturation voltage

Finally, the inversion charge IC is plotted versus the saturation voltage $v_p - v_s$ in Figure 2.6 for both the long- and short-channel cases. We see that velocity saturation reduces the current in strong inversion but has no effect in weak inversion.

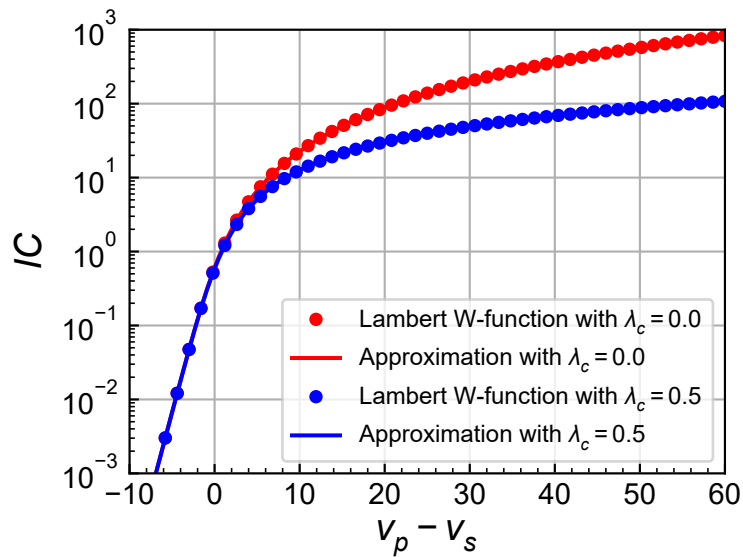


Figure 2.6: Inversion coefficient versus normalized saturation voltage $v_p - v_s$.

2.7 Drain-to-source saturation voltage versus inversion coefficient

The $v_p - v_s$ voltage works well in strong inversion to estimate the saturation voltage for a long-channel transistor. However, it becomes negative in weak inversion and cannot be used for estimating the saturation voltage in weak inversion which should be equal to a few U_T , typically $4U_T$. An approximation of the saturation voltage valid from weak to strong inversion can be defined as

$$v_{dsat} = 2 \sqrt{IC + v_{dsat,wi}^2} \tag{2.21}$$

where $v_{dsat,wi} \cong 4$.

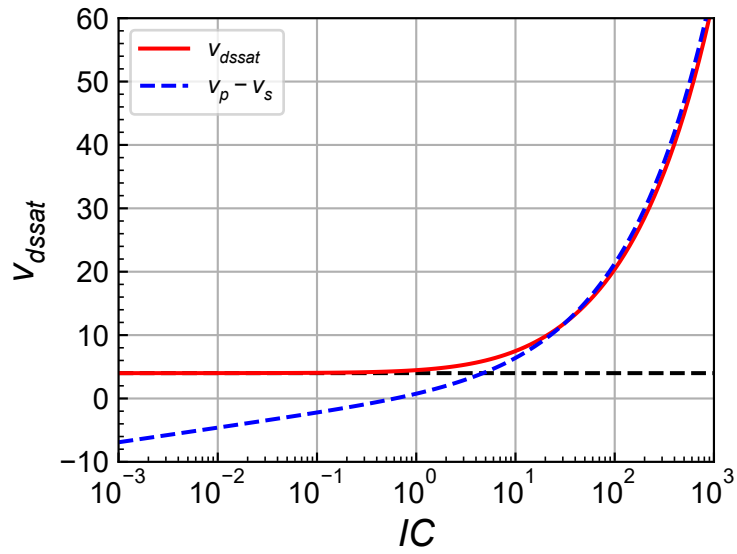


Figure 2.7: Saturation voltage v_{dsat} versus inversion coefficient IC .

2.8 Inversion coefficient versus drain-to-source saturation voltage

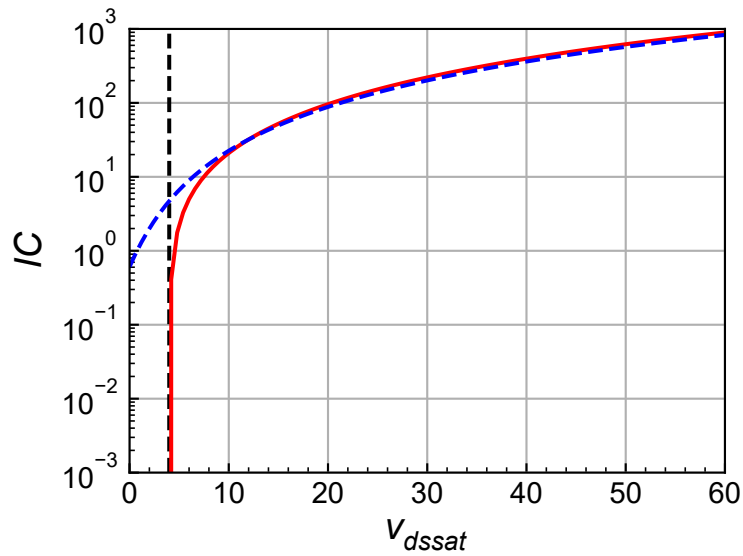


Figure 2.8: Inversion coefficient IC versus saturation voltage v_{dsat} .

2.9 Slope factor versus inversion coefficient

The slope factor n in weak inversion is actually depending on the pinch-off voltage according to

$$n = n_{wi} = 1 + \frac{\Gamma_b}{2\sqrt{\Psi_0 + V_P}} = 1 + \frac{\gamma_b}{2\sqrt{\psi_0 + v_p}} \quad (2.22)$$

where Γ_b is the substrate factor given by

$$\Gamma_b = \gamma_b \cdot \sqrt{U_T} = \frac{\sqrt{2qN_b\epsilon S_i}}{C_{ox}} \quad (2.23)$$

and $\Psi_0 \cong 2\Phi_F +$ a few U_T . The slope factor normally depends on the pich-off voltage which depends on the gate voltage. For $v_s = 0$, we can express the v_p as a function of IC and plot the slope factor versus IC .

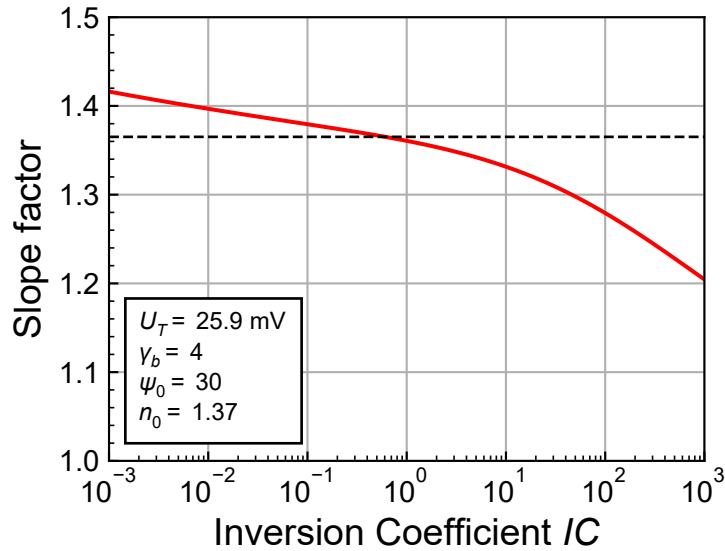


Figure 2.9: Slope factor n versus inversion coefficient IC .

3 Small-signal functions

It can be shown that for a long-channel transistor the source transconductance G_{ms} is actually proportional to the inversion charge taken at the source $Q_i(x=0)$ or to the normalized source charge q_s . The normalized source transconductance g_{ms} can therefore be expressed in terms of the inversion coefficient IC according to

$$g_{ms} \triangleq \frac{G_{ms}}{G_{spec}} = q_s(IC) = \frac{\sqrt{4IC + 1} - 1}{2}, \quad (3.1)$$

where the specific conductance G_{spec} is defined as

$$G_{spec} = \frac{I_{spec}}{U_T} = 2n \cdot \mu \cdot C_{ox} \cdot U_T. \quad (3.2)$$

If velocity saturation is accounted for the normalized source transconductance becomes

$$g_{ms} = \frac{\sqrt{4IC + 1 + (\lambda_c IC)^2} - 1}{2 + \lambda_c^2 IC}. \quad (3.3)$$

The normalized source transconductance in weak and in strong inversion reduces to

$$g_{ms} = \begin{cases} IC & \text{in weak inversion } (IC \ll 1), \\ \frac{1}{\lambda_c} & \text{in strong inversion } (IC \gg 1). \end{cases} \quad (3.4)$$

The normalized source transconductance g_{ms} is plotted versus the inversion coefficient in Figure 3.1 for both the long- and short-channel cases. We see that the normalized source transconductance saturates to $1/\lambda_c$ in SI.

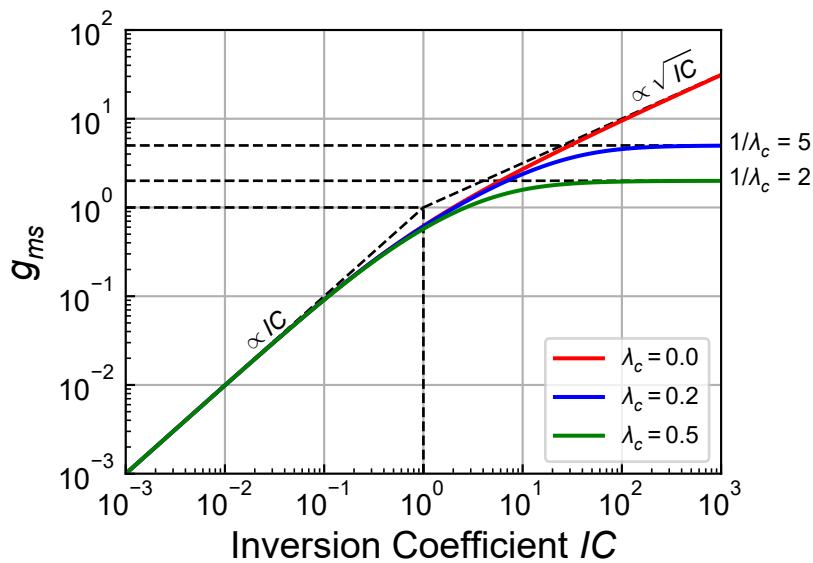


Figure 3.1: Normalized source transconductance g_{ms} versus inversion coefficient IC .

3.1 Inversion coefficient versus transconductance

For long-channel transistor, it is easy to invert the normalized source transconductance to express the inversion coefficient IC required to achieve a given normalized source transconductance

$$IC = g_{ms} \cdot (g_{ms} + 1). \quad (3.5)$$

The formula becomes much more complicated when including velocity saturation. For $\lambda_c > 0$ we get

$$IC = \frac{2 - \lambda_c^2 g_{ms} (1 + 2 g_{ms}) - \sqrt{4 - (\lambda_c g_{ms})^2 (4 - \lambda_c^2)}}{\lambda_c^2 ((\lambda_c g_{ms})^2 - 1)}, \quad (3.6)$$

which for $\lambda_c \rightarrow 0$ reduces to (3.5).

IC is plotted versus g_{ms} in Figure 3.2 for the log- and short-channel cases.

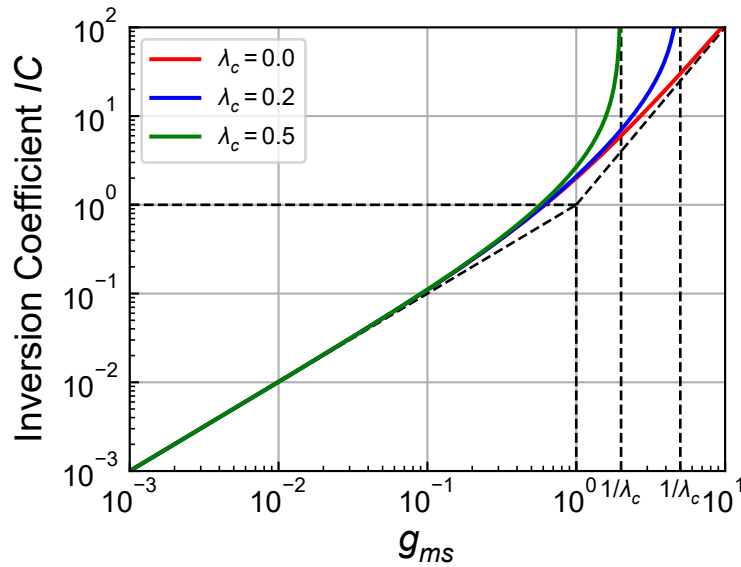


Figure 3.2: Normalized source transconductance g_{ms} versus inversion coefficient IC .

3.2 Normalized G_m/I_D versus inversion coefficient

The normalized G_m/I_D for the long-channel transistor can then be expressed in terms of the inversion coefficient as

$$\frac{G_m \cdot n U_T}{I_D} = \frac{G_{ms} \cdot U_T}{I_D} = \frac{g_{ms}(IC)}{IC} = \frac{\sqrt{4IC + 1} - 1}{2IC} \quad (3.7)$$

For short-channel devices it becomes

$$\frac{G_m \cdot n U_T}{I_D} = \frac{G_{ms} \cdot U_T}{I_D} = \frac{g_{ms}}{IC} = \frac{\sqrt{4IC + 1 + (\lambda_c IC)^2} - 1}{IC(2 + \lambda_c^2 IC)}. \quad (3.8)$$

The normalized source transconductance in strong inversion reduces to

$$\frac{g_{ms}}{IC} = \begin{cases} \frac{1}{\sqrt{IC}} & \text{for long-channel } (\lambda_c = 0), \\ \frac{1}{\lambda_c \cdot IC} & \text{for short-channel } (\lambda_c > 0). \end{cases} \quad (3.9)$$

The normalized G_m/I_D function is plotted below versus IC .

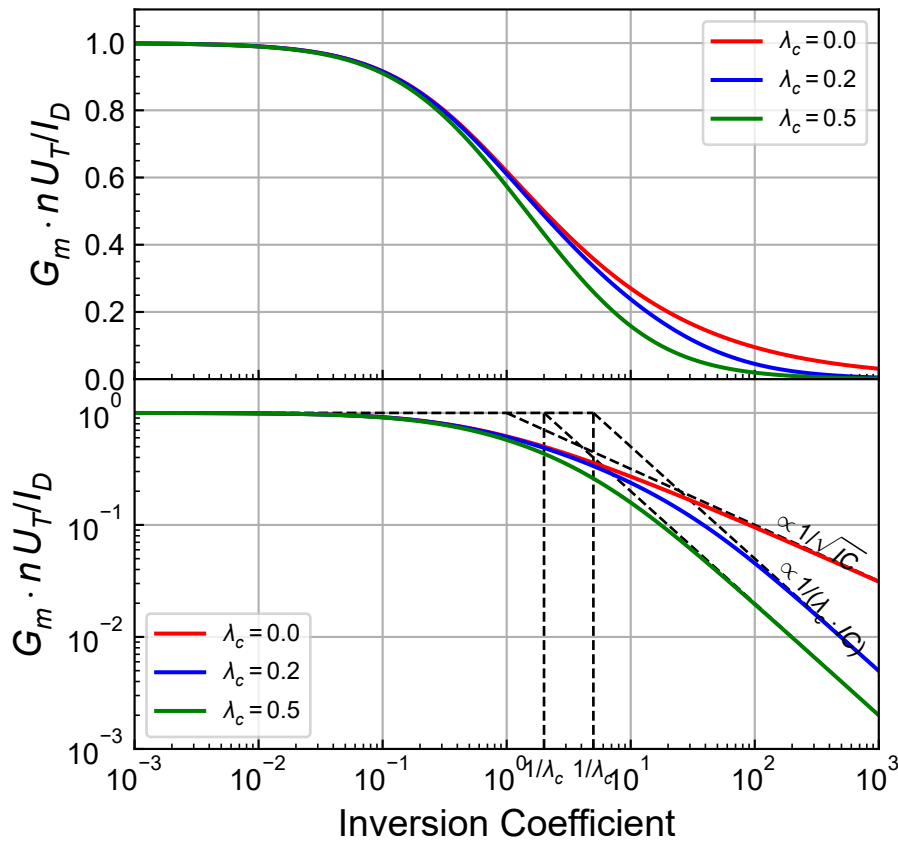


Figure 3.3: Normalized G_m/I_D versus inversion coefficient IC .

3.3 Inversion coefficient versus normalized G_m/I_D

For long-channel transistors, the normalized G_m/I_D can be inverted to express the inversion coefficient as a function of the desired G_m/I_D . This results in

$$IC = \frac{1 - gmsid}{gmsid^2}, \tag{3.10}$$

where $gmsid = G_m nU_T / I_D$.

IC is plotted versus g_{ms}/i_d in Figure 3.4.

There is unfortunately no closed-form expression for the inversion coefficient IC as a function of the normalized G_m/I_D when including velocity saturation. However, it can be solved numerically using `fsolve`.

3.4 Noise functions

3.4.1 Thermal noise

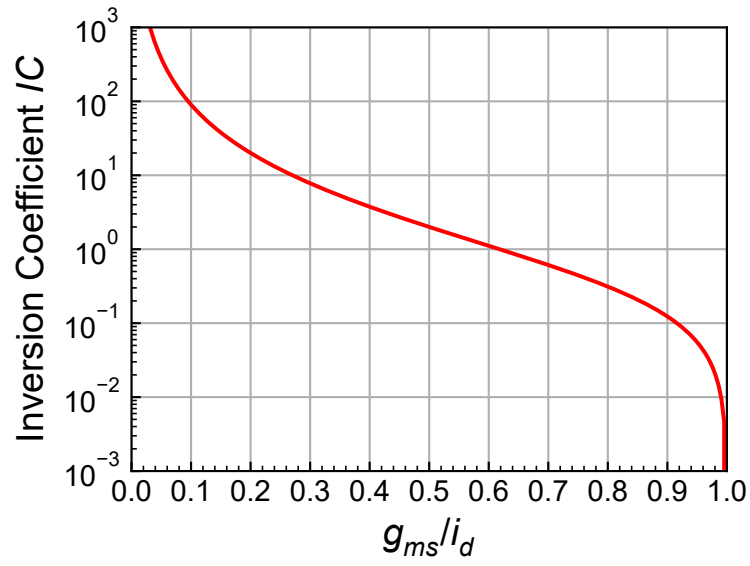


Figure 3.4: Inversion coefficient IC versus normalized G_m/I_D .

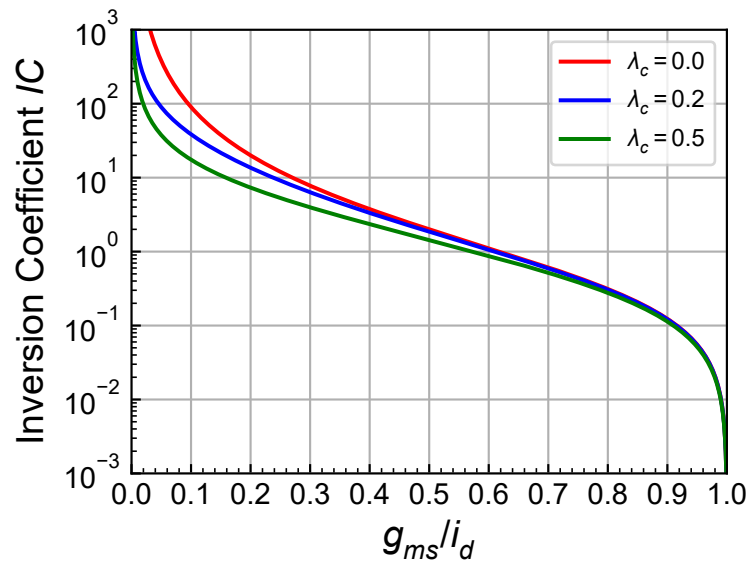


Figure 3.5: Inversion coefficient IC versus normalized G_m/I_D .

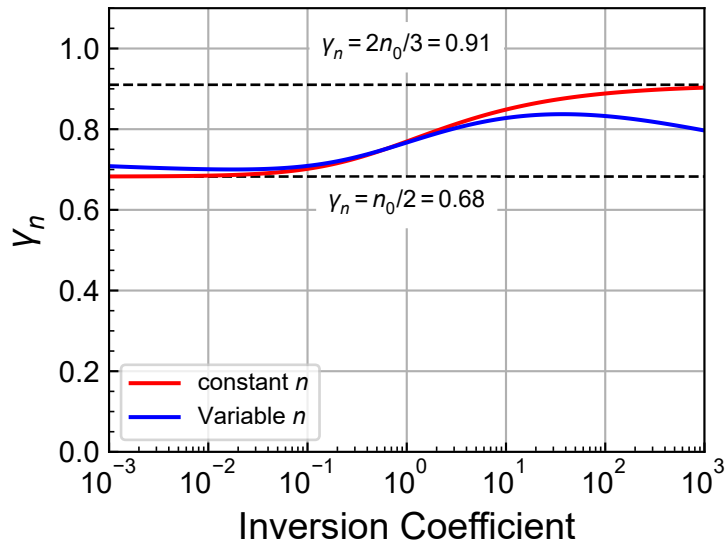


Figure 3.6: Thermal noise excess factor γ_n versus inversion coefficient IC .

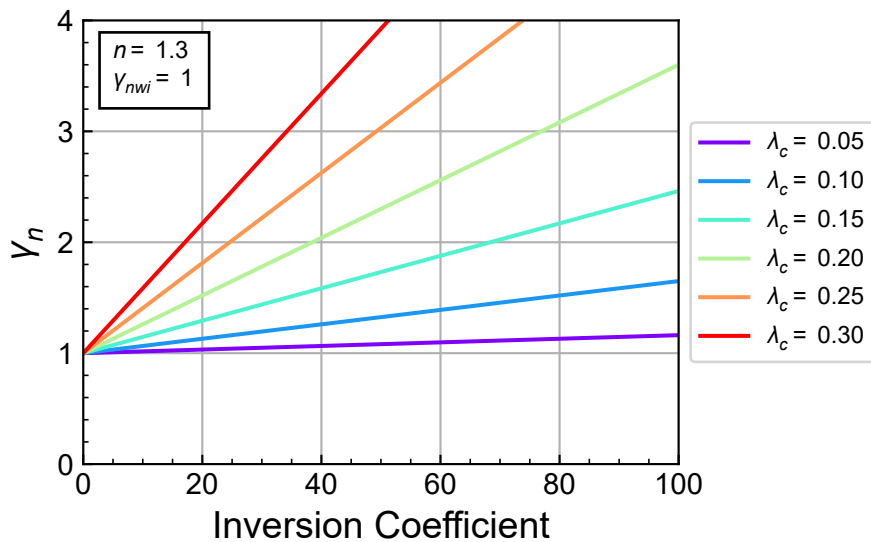


Figure 3.7: Thermal noise excess factor γ_n versus inversion coefficient IC .

4 Normalized intrinsic capacitances

The normalized intrinsic capacitances of a long-channel transistor are given by

$$c_{gsi} \triangleq \frac{C_{GSi}}{C_{OX}} = \frac{q_s}{3} \frac{2q_s + 4q_d + 3}{(q_s + q_d + 1)^2}, \quad (4.1)$$

$$c_{gdi} \triangleq \frac{C_{GDi}}{C_{OX}} = \frac{q_d}{3} \frac{2q_d + 4q_s + 3}{(q_s + q_d + 1)^2}, \quad (4.2)$$

$$c_{gbi} \triangleq \frac{C_{GBi}}{C_{OX}} = \frac{n-1}{n} (1 - c_{gsi} - c_{gdi}), \quad (4.3)$$

$$c_{bsi} \triangleq \frac{C_{BSi}}{C_{OX}} = (n-1) c_{gsi}, \quad (4.4)$$

$$c_{bdi} \triangleq \frac{C_{BDi}}{C_{OX}} = (n-1) c_{gdi}, \quad (4.5)$$

$$c_{ggi} \triangleq \frac{C_{GGi}}{C_{OX}} = c_{gsi} + c_{gdi} + c_{gbi}, \quad (4.6)$$

where $C_{OX} \triangleq W_{eff} L_{eff} C_{ox}$.

The normalized intrinsic capacitances are plotted versus v_p in Figure 4.1. Note that the dashed lines represents the intrinsic capacitances c_{gbi} , c_{bsi} , c_{bdi} and c_{ggi} calculated with a constant slope factor n .

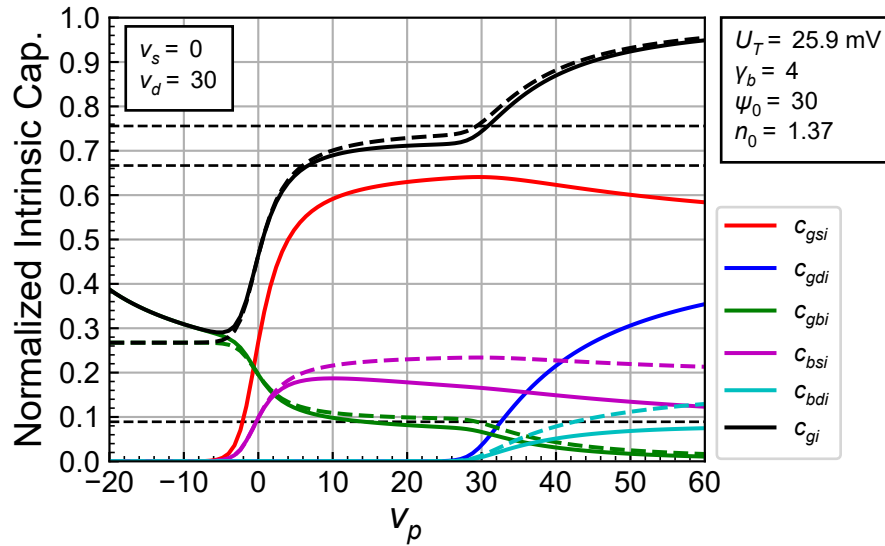


Figure 4.1: Normalized intrinsic capacitance versus normalized pinch-off voltage v_p .

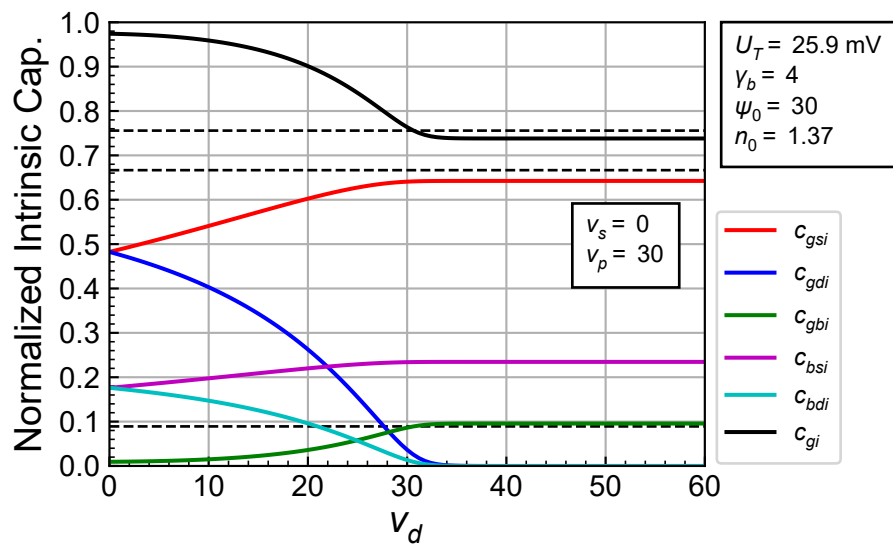


Figure 4.2: Normalized intrinsic capacitance versus normalized drain voltage v_d .

References

- [1] C. C. Enz and E. A. Vittoz, *Charge-Based MOS Transistor Modeling - The EKV Model for Low-Power and RF IC Design*, 1st ed. John Wiley, 2006.
- [2] M. Bucher, C. Lallement, C. Enz, F. Théodoloz, and F. Krummenacher, “The EPFL-EKV MOSFET Model Equations for Simulation.” https://github.com/chrisenz/EKV/blob/main/EKV2.6/docs/ekv_v26_rev2.pdf, 1998.
- [3] C. Enz, F. Chicco, and A. Pezzotta, “Nanoscale MOSFET Modeling: Part 1: The Simplified EKV Model for the Design of Low-Power Analog Circuits,” *IEEE Solid-State Circuits Magazine*, vol. 9, no. 3, pp. 26–35, 2017.
- [4] C. Enz, F. Chicco, and A. Pezzotta, “Nanoscale MOSFET Modeling: Part 2: Using the Inversion Coefficient as the Primary Design Parameter,” *IEEE Solid-State Circuits Magazine*, vol. 9, no. 4, pp. 73–81, 2017.